CellPress

Chemistry & Biology
Article

Targeted Suppression of EVI1 Oncogene Expression by Sequence-Specific Pyrrole-Imidazole Polyamide

Junetha Syed,[1] Ganesh N. Pandian,[2] Shinsuke Sato,[2] Junichi Taniguchi,[1] Anandhakumar Chandran,[1] Kaori Hashiya,[1] Toshikazu Bando,[1] and Hiroshi Sugiyama[1,2,*]

[1]Department of Chemistry, Graduate School of Science, Kyoto University, Sakyo, Kyoto 606-8502, Japan
[2]Institute for Integrated Cell-Material Sciences (iCeMS), Kyoto University, Sakyo, Kyoto 606-8501, Japan
*Correspondence: hs@kuchem.kyoto-u.ac.jp
http://dx.doi.org/10.1016/j.chembiol.2014.07.019

SUMMARY

Human ectopic viral integration site 1 (EVI1) is an oncogenic transcription factor known to play a critical role in many aggressive forms of cancer. Its selective modulation is thought to alter the cancer-specific gene regulatory networks. Pyrrole-imidazole polyamides (PIPs) are a class of small DNA binders that can be designed to target any destined DNA sequence. Herein, we report a sequence-specific pyrrole-imidazole polyamide, PIP1, which can target specific base pairs of the REL/ELK1 binding site in the *EVI1* minimal promoter. The designed PIP1 significantly inhibited EVI1 in MDA-MB-231 cells. Whole-transcriptome analysis confirmed that PIP1 affected a fraction of EVI1-mediated gene regulation. In vitro assays suggested that this polyamide can also effectively inhibit breast cancer cell migration. Taken together, these results suggest that EVI1-targeted PIP1 is an effective transcriptional regulator in cancer cells.

INTRODUCTION

Ectopic viral integration site 1 (*EVI1*) was identified initially as an integration locus of retroviruses in AKXD myeloid tumor mouse models (Mucenski et al., 1988). *EVI1* is a zinc finger transcription regulator encoded in the human chromosome 3q26 that undergoes frequent rearrangements that can activate EVI1 expression in association with pathogenesis caused by myeloid leukemia (Morishita et al., 1992). Ectopic viral integration site 1 plays an important role in hematopoietic stem cell proliferation, and its defects cause deregulated vascularization and neural development during embryogenesis (Hoyt et al., 1997; Yuasa et al., 2005). High expression of EVI1 is categorized as a risk factor for cancer, and several reports have suggested a major role of EVI1 in the onset of leukemic, pancreatic, ovarian, and breast cancers (Brooks et al., 1996; Jazaeri et al., 2010; Lugthart et al., 2008; Tanaka et al., 2014) regardless of the presence of a 3q26 rearrangement. EVI1 coordinates with the proto-oncogene FOS in regulating gene expression to control numerous tumorigenic properties like cellular motility, adhesion, and growth (Bard-Chapeau et al., 2012).

Among the epithelial cancers, breast cancer is the commonly diagnosed malignancy with increasing mortality rate. Robust expression and polymorphism of EVI1 has been reported in breast cancer patients and many breast cancer cell lines (Patel et al., 2011; Wang et al., 2014), and EVI1 influences the cancer risk and prognosis in breast cancer patients. EVI1 is the downstream target of the tumor suppressor microRNA miR-22, and the loss of expression of miR-22 leads to the activation of EVI1-mediated metastasis-specific oncogenic signaling pathways, thus contributing to the pathogenesis of breast cancer cells (Patel et al., 2011). Therefore, development of effectors capable of the targeted repression of EVI1 could be useful in counteracting its tumor-promoting property in the treatment of breast cancer.

The naturally occurring antibiotic distamycin A paved the way for the development of a class of targeting small molecules called pyrrole-imidazole (Py-Im) polyamides (PIPs). PIPs can bind to the DNA minor groove in a sequence-specific mode and compete with the specific transcription factor in binding to their respective DNA recognition sequences. Therefore, polyamides inhibit the DNA-protein interface, causing the modulation in gene expression (Dervan, 2001; Dickinson et al., 1999; Nickols and Dervan, 2007; Trauger et al., 1996; Willis and Arya, 2010). PIPs are synthetic oligomers of N-methylpyrrole and N-methylimidazole that have easy access to cells without the need for a precise delivery system (Bando et al., 2002; Best et al., 2003; Murty and Sugiyama, 2004). PIPs are unaffected by nucleases and are relatively stable inside cells. The pyrrole of PIP prefers binding to T, A, and C bases, whereas the imidazole favors only the G base. Thus, side-by-side pairings of Im/Py and Py/Im in a hairpin bind to G•C and C•G, respectively, whereas Py/Py pairing binds to A•T or T•A. A γ-aminobutyric acid turn in a hairpin PIP selectively prefers A/T, and the paired β-alanine residue (β/β) favors A•T or T•A binding (Bando et al., 2002; Dervan, 2001; Matsuda et al., 2006; Trauger et al., 1996). A hairpin PIP (N to C terminus) generally prefers binding in the 5′-3′ direction of the DNA strand, termed "forward orientation" (White et al., 1997). However, recent studies employing high throughput Bind-n-Seq analysis revealed the N to C aligning of polyamides also in the 3′-5′ direction of the DNA strand, termed "reverse orientation." However, the binding affinity and the orientation preference of the polyamides seem to be completely dependent on its structure-activity relationship that remains to be unsolved (Kang et al., 2014; Meier et al., 2012b).

The ability to regulate gene expression suggests the possible use of hairpin polyamides in medical therapeutics. PIPs

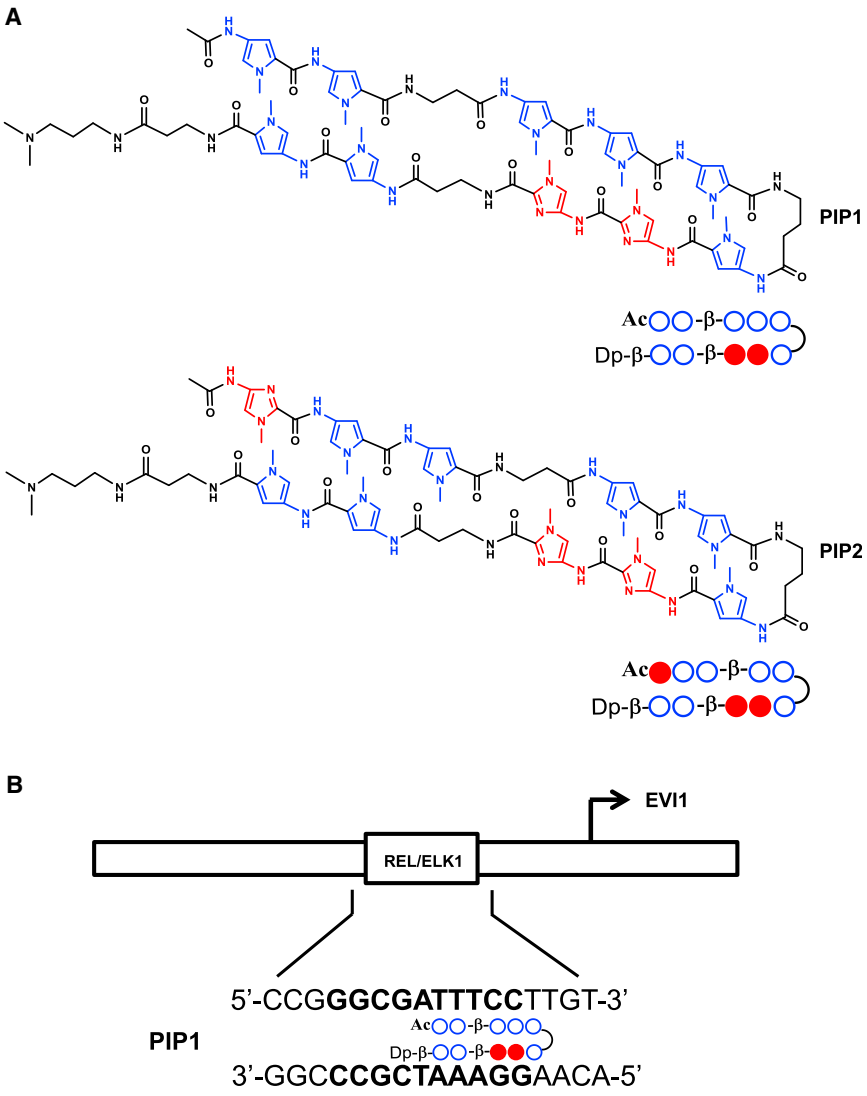

Figure 1. Design of Pyrrole-Imidazole Polyamides

(A) Structures of match polyamide PIP1 and mismatch polyamide PIP2. Pyrrole and imidazole are shown as open and closed circles, respectively.

(B) Schematic representation of the binding of match Py-Im polyamide PIP1 in forward orientation (N- to C-terminal in 5′-3′ direction) to the REL/ELK1 target sequences in the *EVI1* minimal promoter.

designed to bind to the AP-1-binding sequence have been shown to bind to the promoter region of *TGF-β* gene and to reduce TGF-β expression, resulting in improved treatment of progressive renal disease in rat models (Matsuda et al., 2006). The potential application of hairpin polyamides as antitumor agents is a major subject of interest, and several studies have focused on this aspect. Polyamides modulate the expression of downstream genes regulated by androgen, glucocorticoid, and estrogen in cell culture when targeted to their respective consensus response elements (Muzikar et al., 2009; Nickols and Dervan, 2007; Nickols et al., 2013). Hairpin polyamides targeted to the 5′-WGWWCW-3′ sequence significantly reduce tumor growth in mouse xenograft models (Yang et al., 2013). These studies have indicated that polyamides targeted to the gene promoter region may act as an effective gene silencer.

Encouraged by these previous findings, we aimed to produce a hairpin polyamide that could target and inhibit EVI1 expression in the breast cancer cell line MDA-MB-231. Here we show that our synthetic PIP1 targeting the position overlapping the REL and ELK1 recognition sequences in the minimal promoter region of *EVI1* modulates the expression of EVI1. Using genome-wide expression analysis, we found that PIP1 could modulate the downstream targets of EVI1 and the migration of MDA-MB-231 cells. This work reports the ability of a synthetic small molecule to target EVI1. This strategy could be expanded to target critical oncogenic transcription factors of therapeutic importance.

RESULTS

Design of PIPs

ELK1, a member of the ETS family of transcription factors, is one of the major regulators of EVI1 expression (Maicas et al., 2013). Targeting the key sequences like the ELK1 recognition sequence on the promoter region of the therapeutically important factor like *EVI1* could be an efficient way of controlling its expression. In order to obtain the specificity in targeting a particular gene promoter, polyamides have to be designed to cover the boundary that span the consensus sequence recognized by the transcription factor (Matsuda et al., 2006). Specificity toward *EVI1* promoter could be achieved by designing PIPs that cover the overlapping sequences recognized by ELK1 and REL on the human ectopic viral integration site 1 minimal promoter. Such a strategy of targeting overlapping sequences has the advantage of controlling both ELK1 and REL mediated regulation of EVI1 expression. Two nine-base pair-recognizing hairpin PIPs were designed and synthesized to study their effect on the expression of EVI1. We incorporated β/β in the structure of our PIPs because our previous studies have shown that the replacement of pyrrole with β-alanine increases the binding affinity of PIPs to the target DNA sequence (Han et al., 2013). PIP1 was anticipated to bind in the forward orientation 5′-3′ to the targeted REL and ELK1 overlapping bases of the ectopic viral integration site 1 minimal promoter. To substantiate the sequence specificity, PIP2 was designed as a negative control with a single mismatch (a single pyrrole replaced by an imidazole, which interrupts the binding to the match site). Figure 1A shows the structure of the PIP1

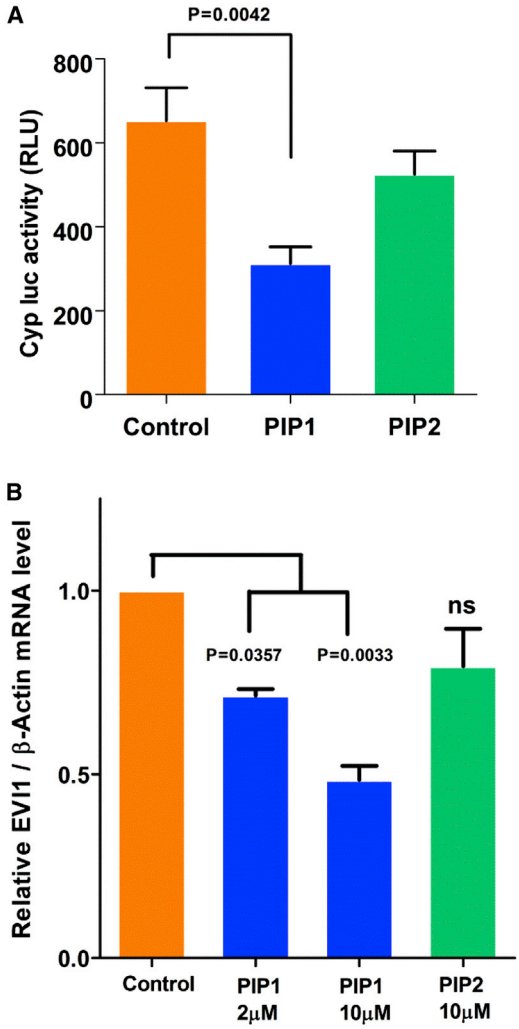

Figure 2. Effect of Polyamide Targeting on Human *EVI1* Promoter Activity and *EVI1* mRNA Expression

(A) MDA-MB-231 cells were transfected with pMCS-Cypridina luciferase vector carrying a human *EVI1* gene promoter insert and treated with DMSO, PIP1, and PIP2 at 2 μm concentration. After 48 hr, *EVI1* promoter activity was measured with the luciferase assay ($p < 0.01$ versus control).

(B) Expression level of *EVI1* mRNA after match forward binding (PIP1) and mismatch (PIP2) treatment in MDA-MB-231 cells by qRT-PCR. The relative expression level of *EVI1* mRNA normalized to β-actin is shown ($p < 0.05$ with respective to the control DMSO). Data are represented as mean ± SEM ($n = 3$).

and PIP2, and Figure 1B depicts the binding of the polyamide matched to its target sequences.

Effect of PIPs on *EVI1* Promoter Activity

We first measured the luciferase activity of the designed PIPs in MDA-MB-231 cells transfected with the human ectopic viral integration site 1 promoter to verify their inhibitory effect. Match hairpin PIP1 significantly repressed the promoter activity by reducing the luciferase emission at 2 μM concentration compared with the control DMSO. By contrast, the mismatch PIP2 (also at 2 μM) had no effect on luciferase activity (Figure 2A).

Quantification of *EVI1* mRNA in PIP-Treated MDA-MB-231 Cells

We next performed quantitative RT-PCR (qRT-PCR) to confirm whether the expression of human ectopic viral integration site 1 mRNA could be modulated by the designed PIPs. The expression level of ectopic viral integration site 1 was significantly inhibited in MDA-MB-231 cells with increasing final concentrations of match PIP1 at concentrations of 2 and 10 μm. However, the mismatch PIP2 (nonsignificant versus control DMSO) did not reduce the *EVI1* mRNA level significantly within the effective concentration range of the match polyamide. This finding confirmed the importance of sequence specificity (Figure 2B).

Genome-wide Profiling of EVI1-Regulated Genes by Match PIPs

We analyzed the global expression changes with the favorable forward-binding PIP1 to verify the biological significance of gene repression. EVI1 is a zinc finger transcription factor that coordinates with various coactivators and corepressors, thereby activating and repressing a large set of functional genes (Izutsu et al., 2001; Soderholm et al., 1997). We next analyzed the comprehensive effect of match PIP1 at a concentration of 10 μM on EVI1-regulated genes using an Affymetrix Human Gene 2.1 ST Array Strip in MDA-MB-231 cells. This array covers about 53,617 gene transcripts. The generated probe set intensity files (CEL files) of the array strips were subjected to the Iter-PLIER algorithm in the core probe set analysis of the Affymetrix expression console software to evaluate the gene level expression measurements. The Iter-PLIER algorithm removes probe sets with unreliable signals and estimates the normalized gene level signal intensities (Huang et al., 2012) after background subtraction in log2scale. To detect the statistically significant changes between DMSO- and PIP1-treated samples, the normalized signal intensities were subjected to t test statistics and the differential expression values were calculated in terms of log 2 ratio. Compared with the control DMSO-treated cells, match PIP1 significantly regulated 985 genes by more than 2-fold, of which 738 genes were downregulated and 247 genes were upregulated (t test, $p < 0.05$).

We then performed gene set enrichment analysis (GSEA) of the significant differentially regulated genes ($p < 0.05$) using the published gene expression profiles in NFS-60 cells after knocking down EVI1 (Glass et al., 2013) with the gene sets (Table S1 available online). GSEA demonstrated that the genes modulated by EVI1-targeted PIP1 showed similarity with the defined EVI1 knockdown gene set (Glass et al., 2013). Furthermore, by assigning the cutoff p value to be less than 0.01 and false discovery rate (FDR) < 0.25, GSEA revealed that the match PIP1 could significantly downregulate the genes upregulated by EVI1 when compared with the control DMSO (Figure 3A). The GSEA-derived heatmap of the EVI1 upregulated genes in the control DMSO and PIP1-treated samples is shown in Figure 3B. Signal intensities are demonstrated by shades of red (upregulation) and blue (downregulation).We also performed qRT-PCR for *PLXNC1* and *LOXL3* as representatives from the GSEA top-ranked list of EVI1 target genes and demonstrated that the expression of the abovementioned genes were modulated only by match PIP1 but not by mismatch PIP2 (Figure S1). This finding indicated the inability of PIP2 to regulate the GSEA-ranked EVI1 target

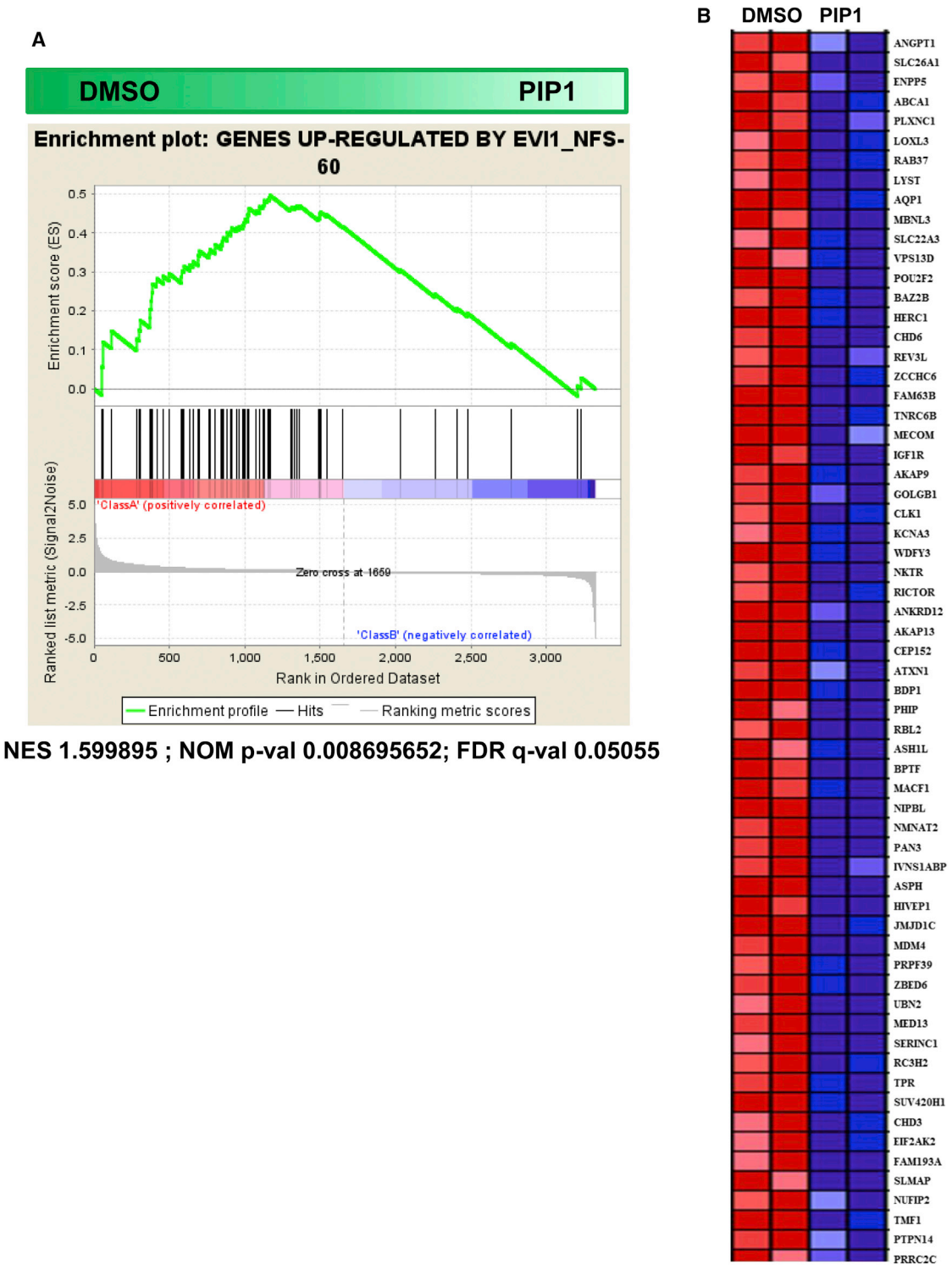

Figure 3. Gene Set Enrichment Analysis

(A) GSEA to conclude whether genes differentially repressed by EVI1 targeted PIP1 (10 μm) were significantly associated with the investigated gene expression profiles (Glass et al., 2013). The enrichment score clearly shows that the genes at the top of the ranked list are overrepresented in the reference gene set. NES, normalized enrichment score; NOM p-val, nominal p value; FDR q-val, false discovery rate q value.

(B) Heatmap of the top ranked genes upregulated in control DMSO (red color) and downregulated in PIP1 samples (blue color), corresponding to the reference gene set.

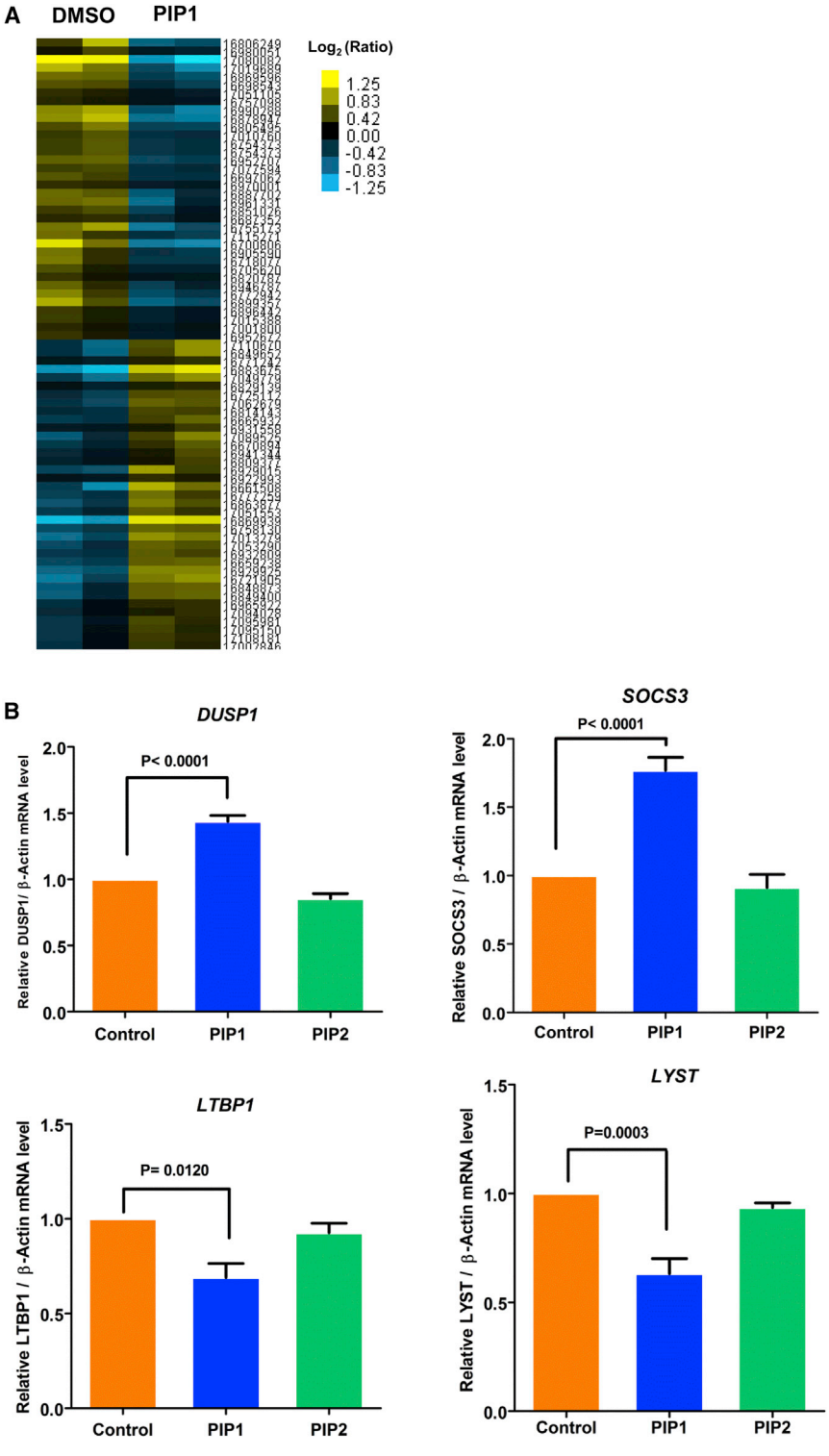

Figure 4. Microarray Analysis of Gene Expression

(A) Heatmap depicting the effect of match Py-Im polyamide 1 on the expression pattern of known EVI1 target genes in the technical duplicates of whole transcriptome analysis ($p < 0.05$) regulated at least 1.2-fold (upregulated value shown in yellow color and downregulated values represented by blue color).

(B) Confirming the effect of Py-Im polyamide 1 (10 μm) in MDA-MB-231 cells observed by whole transcriptome analysis. Relative mRNA levels of four genes (two upregulated [*DUSP1* and *SOCS3*] and two downregulated [*LTBP1* and *LYST*]) were investigated using qRT-PCR ($p < 0.01$ versus DMSO control). Data are represented as mean ± SEM (n = 3).

genes and demonstrated that PIP1 inhibited EVI1 expression and that the observed gene expression profile was due to the modulation by EVI1.

To obtain a deeper insight into the downstream genes differentially regulated by EVI1-targeted PIP1, we next examined the changes in the expression levels of some of the reported EVI1 targets (Bard-Chapeau et al., 2012; Glass et al., 2013; Goyama et al., 2008) and compared these between the DMSO- and PIP1-treated microarray expression profile data using a heatmap. Heatmaps are employed to display the signal intensities of gene probes in colored cells, where strong signal intensities (highest expression value) are represented by yellow or red and where blue represents the weak intensity (lowest expression value), whereas the intermediate probe expression values are indicated by varying shades of yellow/red and blue. This analysis included the genes that were significantly regulated (t test, $p < 0.05$) by >1.2-fold by match PIP1. The heatmap image generated to represent the differentially expressed signatures of the known EVI1-regulated genes in PIP1-treated samples relative to the expression in the control DMSO-treated samples is shown in Figure 4A. The analysis revealed that match PIP1 downregulated those genes upregulated by EVI1 and that PIP1 also upregulated the EVI1-repressed genes. The genes represented in the heatmap and their respective fold changes are shown in Tables 1 and S2.

Some of the representative upregulated genes (*DUSP1* and *SOCS3*) and downregulated genes (*LTBP1* and *LYST*) were selected for qRT-PCR to verify the microarray expression data obtained for PIP1. The observed results demonstrated that the match PIP1 effectively reproduced the gene regulation in a pattern similar to that of the microarray data, whereas mismatch PIP2 failed to regulate the EVI1 target genes (Figure 4B). These results explain that PIP1 gains over the mismatch PIP2 in the specificity toward targeting EVI1 and its downstream genes.

Table 1. Expression Pattern of EVI1 Downstream Genes Regulated by PIP1 in MDA-MB-231 Cells

Transcript ID	Gene Symbol	Fold Change[a]	p < 0.05[b]
16883675	*IL1RL2*	3.20025419	0.011043493
16869939	*UCA1*	3.197761186	0.004433311
16661508	*SMPDL3B*	2.053481144	0.04528849
16721905	*ADM*	1.969589943	0.017152285
16929925	*GCAT*	1.943088619	0.001396785
17013279	*STX11*	1.933034786	0.009880415
17049779	*SH2B2*	1.855266966	0.029205669
17110670	*PIM2*	1.769033048	0.04284442
16929015	*OSBP2*	1.753892713	0.04055794
16849652	*TBC1D16*	1.73395493	0.047790155
16863877	*PPP1R15A*	1.689966678	0.017193692
17089525	*LCN2*	1.663160961	0.035273492
16849400	*SOCS3*	1.6559035	0.024376618
16659238	*TNFRSF1B*	1.646927446	0.000786928
16848873	*GALK1*	1.639203875	0.023774723
16758130	*ORAI1*	1.63325154	0.004703509
17062679	*IMPDH1*	1.616689923	0.01009058
16772942	*ZMYM2*	−1.633062493	0.04165688
16952707	*ZNF445*	−1.638142318	0.001358996
16887702	*ITGA6*	−1.639071739	0.025391394
16805495	*IGF1R*	−1.655426434	0.008250059
16869596	*LPHN1*	−1.690483225	0.004838508
16961331	*MECOM*	−1.723875995	0.042155035
16806249	*OCA2*	−1.88105574	0.04891156
16899357	*LOXL3*	−1.88830211	0.03693188
16755173	*PLXNC1*	−1.994683293	0.015575908
17019689	*ENPP5*	−2.098588493	0.033430777
16990288	*PCDHB16*	−2.108754723	0.014634904
16878947	*LTBP1*	−2.282375238	0.00473262
16700806	*LYST*	−2.446506812	0.03618726
17080082	*ANGPT1*	−6.098613551	0.04926165

[a]Fold change of the activated and repressed downstream target genes of EVI1 more than 1.6-fold by match PIP1 with respect to the control.
[b]The p value was calculated using t test statistics by the MeV microarray data analysis platform. $p < 0.05$ is considered to be statistically significant.

We also performed ingenuity pathway analysis (IPA) of the differentially expressed genes to gain a more precise global understanding of the underlying biological processes. Interestingly, in this analysis, the large number of genes corresponding to functions such as homing of cells, metastasis, lymphoma adhesion, and cell maturation were downregulated. EVI1 functions as a survival factor and brings resistance to cell death (Liu et al., 2006), and it also promotes cell proliferation by modulating the expression of growth-stimulating factors (Gómez-Benito et al., 2010; Nayak et al., 2013). The IPA analysis of the microarray data also revealed that most genes related to organismal death and growth failure were upregulated to suggest the role of EVI1-targeted PIP1 in inducing apoptotic cell death and inhibiting the cellular proliferation, respectively. The abovementioned functional annotations were highly enriched in the genes differentially regulated by PIP1 compared with the DMSO-treated control (Table 2). In the IPA, *Z* scores above (activation) and below (inhibition) the value of two were statistically significant.

Biological Evaluation of PIP1 Reveals Antitumor Activities

To verify whether the changes in gene expression are manifested in changes in biological activity, we evaluated the ability of PIP1 to inhibit the migration of MDA-MB-231 cells in a scratch wound-healing assay. The DMSO-treated control tumor cells induced the complete closure of the wound area within 24 hr, whereas treatment with PIP1 at 2 μM efficiently hindered the migration of the breast cancer cells compared with PIP2 (Figure 5A).

To determine whether EVI1-targeted PIP1 can affect cancer cell invasion, we performed an invasion assay by incubating MDA-MB-231 cells with DMSO, PIP1, or PIP2 at 2 μM for 24 hr. PIP1 reduced the number of cells invading across Matrigel, but DMSO and PIP2 had no significant effect on cell invasion (Figures 5B and 5C).

An in vitro cell proliferation assay was performed to assess the effect of PIP1 on cell growth. MDA-MB-231 cells were treated with PIP1 at various concentrations and incubated for 72 hr. The WST8 assay showed that PIP1 exhibited a mild range of cytostatic activity in a concentration-dependent manner (Figure 5D).

DISCUSSION

PIPs have the unique property of being able to recognize nucleic acid base sequences by following the proposed DNA-recognition rule (Geierstanger et al., 1994; Trauger et al., 1996; White et al., 1996). PIPs can bind to a specific predetermined sequence wrapped inside nucleosomes and can influence chromatin structure. The prospective application of PIPs in gene therapy relies on their controlled sequence specificity (Bando et al., 2002; Dervan, 2001; Matsuda et al., 2006; Nickols and Dervan, 2007; Nickols et al., 2013; Ueno et al., 2009; Yang et al., 2013). Human cancer is often associated with overexpression of tumor inducing genes; under such conditions, PIPs have the potential use as novel antitumor agents as they can prevent the enhanced expression of the target gene by interfering with the binding of transcription factors to their respective regulatory sequences without affecting the basal expression needed for the normal cellular function (Takahashi et al., 2008). Several recent investigations have focused on the antitumor properties of PIPs (Nickols and Dervan, 2007; Nickols et al., 2013; Wang et al., 2010; Yang et al., 2013).

The transcriptional activity of the highly conserved oncoprotein EVI1 is regulated by phosphorylation at serine 196 in its first zinc finger domain (White et al., 2013). Elevated expression of EVI1 results in the malignant transformation of many epithelial cells as breast, ovarian, and pancreatic cancers (Brooks et al., 1996; Jazaeri et al., 2010; Lugthart et al., 2008; Tanaka et al., 2014; Patel et al., 2011). Many basal and BRCA1 associated breast tumors have been correlated with the overexpression of EVI1 in comparison with the normal breast tissue (Weber-Mangal

Table 2. Significantly Enriched Biological Functional Annotation by IPA

Category	p Value [a]	Functions Annotation[b]	Predicted Activation State	Activation *Z* Score[c]	Number of Molecules
Organismal survival	7.22×10^{-4}	organismal death	increased	3.394	204
Developmental disorder	1.29×10^{-2}	growth failure	increased	2.620	56
Hematological system development and function	3.79×10^{-5}	quantity of blood cells	decreased	−3.937	104
Cellular movement	1.12×10^{-2}	chemo taxis of cells	decreased	−2.778	46
	6.16×10^{-3}	homing of cells	decreased	−2.606	50
Cell-to-cell signaling and interaction	6.86×10^{-3}	adhesion of lymphoma cell lines	decreased	−2.581	7
Cancer	2.72×10^{-4}	metastasis	decreased	−2.066	65
Cellular development	4.62×10^{-3}	maturation of cells	decreased	−2.050	40

[a]The p value is determined by the likelihood of the number of focus genes associated with a particular biological process. p value < 0.05 is considered to significant.
[b]Functional annotation is assigned based on the literature deposited in the IPA knowledge base.
[c]A positive *Z* score suggests the potential activation, and a negative *Z* score refers to the potential inhibition of the particular functional process.

et al., 2003; Wessels et al., 2002). Also, EVI1 is known to be associated with reduced metastasis-free and overall survival rates of ERα-positive subgroups of breast cancer patients. The abnormal expression of EVI1 is the result of its genetic variants, and it may offer resistance toward chemotherapy, resulting in the breast cancer patient relapse (Patel et al., 2011). Recent population studies of breast cancer patients revealed the existence of EVI-1 rs6774494 polymorphism that is responsible for the etiology of breast cancer (Wang et al., 2014). This aberrant expression of EVI1 in carcinogenic conditions is governed by the transcription factors ELK1 and RUNX1 by binding to their respective regulatory sequences on the *EVI1* minimal promoter region (Maicas et al., 2013).

Accumulating evidence indicates that EVI1 overexpression plays an important role in malignancy and has prompted an interest in developing inhibitors against EVI1 as targeted cancer therapy. At present, small interfering RNA therapeutics is the only available option to treat EVI1-associated diseases. However, nucleic acid medicines have the disadvantages that they can be degraded easily by nucleases and that they require efficient delivery systems to reach their designated targets (Takahashi et al., 2008). PIPs obviate these drawbacks because they can permeate into the nuclei of living cells (Best et al., 2003) and are highly resistant to nuclease digestion.

In our study, PIP1 (forward 5′-3′ binding) designed to cover the overlapping ELK1 and REL recognition sequences on the *EVI1* promoter reduced the promoter activity by decreasing the luciferase emission and also inhibited the expression of EVI1. Since polyamides can also align in the reverse orientation to the DNA (Kang et al., 2014; Meier et al., 2012b), we evaluated the ability of a polyamide (PIP3) designed to bind in the 3′-5′ orientation to the target *EVI1* promoter sequence (Figure S2A) in inhibiting EVI1 expression. As expected, a significant inhibitory effect of PIP3 could be observed on the EVI1 expression (Figure S2B). Our study could contribute to the future studies focusing on the importance of PIP binding preferences, which in turn could aid the development of efficient PIPs for gene regulation in targeted therapeutics. Zhang et al. (2011) previously developed polyamides to target the DNA motif recognized by EVI1. However, in this study only the in vivo EVI1 responsive reporter activity assay was done to prove that the polyamide could block the binding of EVI1 to the DNA and inhibit the EVI1 mediated transcription activity (Zhang et al., 2011). Herein, we substantiated the scope of previous work by developing a polyamide PIP1 capable of significantly inhibiting the expression of EVI1 itself. Furthermore, through genome-wide transcriptome analysis we have demonstrated in a cell culture model that PIP1 at a concentration of 10 μM can modulate a fraction of EVI1-driven transcription of its target genes. These results demonstrate that MDA-MB-231 cells effectively took up EVI1 targeting PIP1 and that they could bind to the target sequence, resulting in the reduction of EVI1 and its downstream genes expression.

In the IPA analysis, the biological process enriched in the regulated transcripts suggested that PIP1 is involved in the negative regulation of cell movement, cell survival, and cellular growth. The contributory role of ectopic viral integration site 1 in metastasis is supported by growing evidence. EVI1 has been shown to contribute to the epithelial-mesenchymal transition (EMT) to promote the migration potential of breast and ovarian cancer cells (Dutta et al., 2013). The epigenetic control possessed by EVI1 is considered to be responsible for the adaptation of the breast cancer cells in the metastatic sites (Patel et al., 2011). Several reports have demonstrated that EVI1 protects cells from programmed cell death (Liu et al., 2006; Pradhan et al., 2011). Interestingly, in our experiments PIP1 targeting the ectopic viral integration site 1 reduced the cell migration as well as induced more apoptosis (Annexin V staining; Figures S3A and S3B) when compared with the control DMSO and mismatch polyamide PIP2. Ectopic viral integration site 1 stimulates cell proliferation (Gómez-Benito et al., 2010; Nayak et al., 2013), but the level of effect completely varies between cell types (Wieser, 2007). For example, in Rat-1 fibroblasts, murine myeloid, and embryonic stem cells (Chakraborty et al., 2001; Kilbey et al., 1999; Sitailo et al., 1999), EVI1 plays an important role in controlling the cell proliferation, whereas in REH cells, ectopic viral integration site 1 displays a weak proliferative activity (Konantz et al., 2013). The mechanism of EVI1

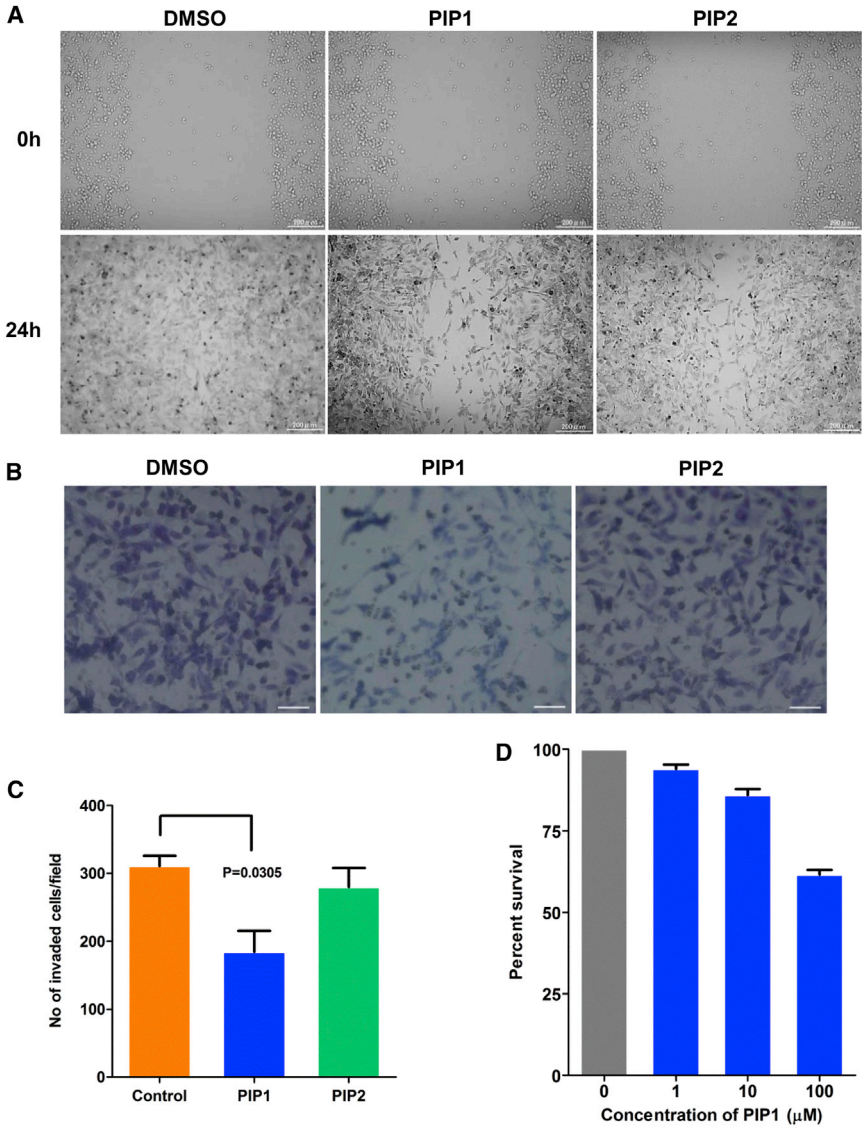

Figure 5. Biological Activity of Match PIP1

(A) In vitro cell migration of the MDA-MB-231 cells. Cells were wounded with tips of micropipette and treated with DMSO, PIP1, and PIP2. The extent of wound closure was photographed after 24 hr (upper panel at 0 hr and lower panel at 24 hr). Scale bars represent 200 μm.

(B) In vitro invasion assay of the MDA-MB-231 cells across the Matrigel coated membrane with or without polyamide treatment. Scale bars represent 100 μm.

(C) Quantification of the cells migrated through the Matrigel ($p < 0.05$ versus control).

(D) WST 8 assay to measure the percentage of breast cancer cell survival after 72 hr post treatment with PIP1. Values are represented as mean ± SEM (n = 3).

in the control of cellular proliferation remains inconclusive due to these conflicting reports. Already reported polyamide designed to inhibit the binding of EVI1 to DNA also exhibited partial inhibition of leukemic cell growth (Zhang et al., 2011). This context-dependent behavior of EVI1 on cell growth may demonstrate the weak antiproliferative effects of EVI1-targeted PIP1 even at 100 μM concentration in MDA-MB-231 cells. The mode of action of many cancer drugs targeting DNA is nonspecific, resulting in undesirable cytotoxicity and the potential development of secondary malignant tumors (Arseneau et al., 1972; Yang et al., 2013). Therefore, the tailor-made PIP1 could be a promising agent in targeting EVI1 and its corresponding context-dependent downstream effects.

While developing potent antitumor drugs, their solubility is an important factor to be considered with respect to the adverse toxicity. Polyamides have been reported to exhibit limited or no cytotoxicity in mouse xenograft models and cell cultures (Wang et al., 2010; Yang et al., 2013). However, some pyrrole-imidazole polyamides can form aggregates at higher concentration. Thus, optimizing their structure can improve their solubility and biological activity (Meier et al., 2012a; Hargrove et al., 2012). Prospective studies on the solubility and pharmacokinetic behavior of the EVI1-targeted PIP1 will be helpful in evaluating its therapeutic potential.

The potential applications of these EVI1-targeted PIPs in future therapeutics will depend on the effects of this small molecule in animal model experiments. Future investigations should include efforts to optimize the reported hairpin PIP structures to improve their specificity toward inhibition of EVI1 expression. Target sequences recognized by other transcription factors in the regulation of ectopic viral integration site 1 expression cannot be ruled out when designing more effective hairpin PIPs for targeted therapy (Warren et al., 2006). On the basis of these findings, future studies should address the possible applications of this DNA-binding small molecule as an effective gene silencer to treat EVI1-associated tumorigenesis.

SIGNIFICANCE

In our study, we have developed a potent small molecule PIP1, targeting the human ectopic viral integration site 1 (*EVI1*) promoter. The designed polyamide was found to significantly reduce the *EVI1* mRNA level, indicating that PIP1 interfere with the protein binding to its regulatory sequence. EVI1 is an oncogenic transcription regulatory protein governing a wide range of potential tumor genes, and as expected PIP1 exerted its effect on some of the EVI1-regulated downstream genes like *LOXL3*, *LTBP1*, etc., which play a major role in tumor development. In addition, PIP1 exhibited potent antimetastatic properties MDA-MB-231 breast cancer cells. These results propose that PIP1 may be a selective silencer of EVI1 and stimulates new prospects

to develop novel antitumor agents based on the molecular recognition ability of pyrrole-imidazole polyamides.

EXPERIMENTAL PROCEDURES

Polyamide Synthesis

The synthesis of polyamides 1 to 3 was performed on a PSSM-8 peptide synthesizer (Shimadzu) with a computer-assisted operation system by using Fmoc chemistry as previously reported (Bando et al., 2002). Reaction steps in the synthetic cycle were as follows: deblocking steps by piperidine in dimethylformamide (DMF); a coupling step with corresponding carboxylic acids by 1H-Benzotriazolium 1-[bis(dimethylamino)methylene]-5chloro-,hexafluorophosphate (1-),3-oxide (HCTU), N,N-Diisopropylethylamine, and N-Methyl-2-pyrrolidone (NMP); and washing steps by DMF. Each coupling reagents in steps were prepared in DMF solution of Fmoc-Py-COOH, Fmoc-I-COOH, Fmoc-PyIm-COOH, Fmoc-β-COOH, and Fmoc-γ-COOH. All other couplings were carried out with single-couple cycles with stirred by N_2 gas bubbling. Typically, Fmoc-Py loaded oxime-acid resin (40 mg, ca. 0.2 mmol/g, 200∼400 mesh) was swollen in 1 ml of DMF in a 2.5 ml plastic reaction vessel for 30 min. Two-milliliter plastic centrifuge tubes with loading Fmoc-monomers with HCTU in NMP 1 ml were placed in order position. After the completion of the syntheses on the peptide synthesizer, the resin was washed with a mixture of methanol (2 mL) and dried in a desiccator at room temperature in vacuum. After the cleavage from the resin by dimethylaminopropane, the crude was purified by flash column chromatography to obtain the desired Py-Im polyamides 1–3. Analytical high-performance liquid chromatography and MALDI-TOF mass spectrometry was conducted to confirm the purity of the compounds.

Cell Culture

MDA-MB-231 (breast, human) cell line was purchased from European collection of cell cultures. Cells were grown in Dulbecco's modified Eagle's medium (DMEM) supplemented with 10% fetal bovine serum (FBS), 100 U/mL penicillin, and 100 μg/mL streptomycin at 37°C in 5% CO_2 (Wang et al., 2010).

Luciferase Assay

To determine the effect of Py-Im polyamides on *EVI1* promoter, the human *EVI1*-promoter-pMCS Cypridina luciferase reporter (Thermo Scientific) chimeric plasmid was constructed to perform the luciferase reporter assay. The primers used in the *EVI1* promoter cloning are listed in Table S3. MDA-MB-231 cells were seeded in 24-well plates at 8 × 10^4 cells/well. The reported plasmid containing the *EVI1* promoter (1 μg) was transfected into the cells using FuGENE 6 transfection reagent (Promega). After 2 hr the cells were treated with 2 μM Py-Im polyamide. The luciferase activity was measured after 48 hr with Pierce Cypridina luciferase Flash Assay Kit (Thermo Scientific) at 463 nm using a Spectra Max 190 (Molecular Devices) microplate reader.

Quantitative Reverse-Transcription PCR

MDA-MB-231 cells were plated in 6-well plates at 2 × 10^5 cells/well and were treated with various concentrations of Py-Im polyamide for 48 hr. Cells treated with DMSO are represented as control samples. Total RNA was extracted using an RNEasy Kit (QIAGEN), and cDNA was synthesized by a ReverTra Ace qPCR RT Kit (Toyobo) according to the manufacturer's instructions. The expressions of mRNA were analyzed by an ABI 7300 Real Time PCR system (Applied Biosystems) using Thunderbird SYBR q-PCR mix (Toyobo). The delta Ct (ΔCt) method was used to analyze the qRT-PCR data. The expression level of the β-actin gene was used as the internal control to normalize the target mRNA expression. The primer list used for performing qRT-PCR is given in the Table S3.

Microarray Analysis

MDA-MB-231 cells were plated in 6-well plates at 2 × 10^5 cells/well and were treated for 48 hr with DMSO (0.005% control) and 10 μM concentration of PIP1, with technical duplicates in each condition respectively. Total RNA was prepared and the integrity of the RNA was checked using the Agilent 2100 Bioanalyzer (Agilent Technologies). One hundred nanograms of total RNA quantified by Nanodrop ND1000 v. 3.5.2 (Thermo Scientific) was labeled using a GeneChip WT PLUS Reagent kit (Affymetrix) and was hybridized to Human Gene 2.1 ST Array Strip (Affymetrix) for 20 ± 1 hr at 48°C. The hybridized arrays were washed, stained, and imaged on a GeneAtlas Personal Microarray System (Affymetrix). The hybridized probe set values were normalized using Affymetrix gene expression console software and analyzed for gene expression using the MultiExperiment Viewer (MeV) microarray data analysis platform (http://www.tm4.org/mev.html). Significant differentially expressed genes between the different conditions were analyzed using t test statistics ($p < 0.05$). The heatmap of the differentially regulated genes was generated using Cluster 3.0 and Java Tree View software. Microarray data reported here were deposited in the Gene Expression Omnibus database under the accession number GSE59502.

Data Analysis

Gene set enrichment analysis (GSEA; Subramanian et al., 2005) was conducted using GSEA v. 2.0.14 software to detect statistically significant PIP 1 targeted genes associated with a gene set containing EVI1-regulated genes. Data were further analyzed by IPA (Ingenuity Systems; http://www.ingenuity.com). The IPA functional analysis was conducted to identify the significant biological functions associated with the microarray data set. Genes from the data sets that were regulated by ≥1.5-fold cutoff at $p < 0.05$ were considered for the analysis. The p value was calculated using right-tailed Fisher's exact test that defines the degree of association of the data set to the assigned biological function.

Scratch-Wound Migration Assay

MDA-MB-231 cells were seeded in an 8-well chamber slide at 3 × 10^5 cells/well. The cell layers were wounded with a large orifice plastic micropipette in order to measure the cell migration during wound healing. The medium with the cell debris was removed and supplemented with 400 μl of fresh medium containing 2 μM Py-Im polyamide. Cells treated with DMSO (0.005%) were used as control. Diff-Quik solution (Kokusaishiyaku) was used to stain the cells at 24 hr after wounding and images were captured by phase-contrast microscopy (Biorevo, BZ-9000, Keyence).

Matrigel Invasion Assay

BioCoat Matrigel Invasion Chambers (BD Bioscience) comprising transwell (8-μm pore-sized membranes coated with Matrigel) filter inserts in a 24-well tissue culture plate were used to evaluate cell invasion. The upper chamber was placed with MDA-MB-231 (5 × 10^4 cells/well) suspended in 300 μl of DMEM medium + 0.1% FBS containing 2 μM concentration of PIPs and 700 μl DMEM medium containing 5% FBS was added in the lower well. After 24 hr of incubation the noninvaded cells on the upper surface of the filter were wiped out with a cotton swab, and cells that invaded across the Matrigel were fixed and visualized using Diff-Quik solution staining.

In Vitro Cell Proliferation

MDA-MB-231 cells were seeded on 96-well microplates (5 × 10^3 cells/well) and treated with diverse concentrations of PIPs and then incubated for 72 hr at 37°C in 5% CO_2. Count Reagent SF (Nacalai Tesque) was added to each well to evaluate the cell proliferation. The absorbance of each well was measured at 450 nm by an MPR-A4iII (Tosoh) microplate reader (Wang et al., 2010).

Apoptosis Detection Assay

The apoptosis detection assay was performed using an Apoptotic, Necrotic, and Healthy Cells Detection Kit (Promokine) according to manufacturer's instructions. MDA-MB-231 cells were cultured in 8-well chamber slides at a density of 2 × 10^4 cells/well and treated with 2 μM Py-Im polyamide for 48 hr. The cells were washed with a binding buffer and stained with FITC-Annexin V, Ethidium Homodimer III, and Hoechst 33342 (Firat et al., 2012); then they were subjected to fluorescence microscopy analysis (Biorevo, BZ-9000, Keyence), and the images were processed by BZ-II analyzer software. The percentage of apoptotic cells were calculated by the number of Annexin V positive cells/total number of cells × 100.

Statistical Analysis

Results are expressed as mean values ± SEM. Statistical significance was determined by one-way ANOVA, followed by the Tukey's multiple comparison test. The p values less than 0.05 were considered to be significant.

SUPPLEMENTAL INFORMATION

Supplemental Information includes three figures and three tables and can be found with this article online at http://dx.doi.org/10.1016/j.chembiol.2014.07.019.

AUTHOR CONTRIBUTIONS

Experiments were designed by H.S., J.S., T.B., and G.N.P. Research was performed by J.S. K.H. synthesized Py-Im polyamides. J.S., S.S., J.T., and A.C. analyzed the data. The manuscript was written by J.S. and G.N.P.

ACKNOWLEDGMENTS

This work was supported by the Ministry of Education, Culture, Sports, Science and Technology (MEXT) of Japan, administrated by the Japan Society for the Promotion of Science. J.S. is thankful to Japan Educational Exchange and Services (JEES) and Mitsubishi Corporation for providing scholarships.

Received: June 5, 2014
Revised: July 11, 2014
Accepted: July 15, 2014
Published: September 11, 2014

REFERENCES

Arseneau, J.C., Sponzo, R.W., Levin, D.L., Schnipper, L.E., Bonner, H., Young, R.C., Canellos, G.P., Johnson, R.E., and DeVita, V.T. (1972). Nonlymphomatous malignant tumors complicating Hodgkin's disease. Possible association with intensive therapy. N. Engl. J. Med. *287*, 1119–1122.

Bando, T., Narita, A., Saito, I., and Sugiyama, H. (2002). Molecular design of a pyrrole-imidazole hairpin polyamides for effective DNA alkylation. Chemistry *8*, 4781–4790.

Bard-Chapeau, E.A., Jeyakani, J., Kok, C.H., Muller, J., Chua, B.Q., Gunaratne, J., Batagov, A., Jenjaroenpun, P., Kuznetsov, V.A., Wei, C.-L., et al. (2012). Ecotopic viral integration site 1 (EVI1) regulates multiple cellular processes important for cancer and is a synergistic partner for FOS protein in invasive tumors. Proc. Natl. Acad. Sci. USA *109*, 2168–2173.

Best, T.P., Edelson, B.S., Nickols, N.G., and Dervan, P.B. (2003). Nuclear localization of pyrrole-imidazole polyamide-fluorescein conjugates in cell culture. Proc. Natl. Acad. Sci. USA *100*, 12063–12068.

Brooks, D.J., Woodward, S., Thompson, F.H., Dos Santos, B., Russell, M., Yang, J.M., Guan, X.Y., Trent, J., Alberts, D.S., and Taetle, R. (1996). Expression of the zinc finger gene EVI-1 in ovarian and other cancers. Br. J. Cancer *74*, 1518–1525.

Chakraborty, S., Senyuk, V., Sitailo, S., Chi, Y., and Nucifora, G. (2001). Interaction of EVI1 with cAMP-responsive element-binding protein-binding protein (CBP) and p300/CBP-associated factor (P/CAF) results in reversible acetylation of EVI1 and in co-localization in nuclear speckles. J. Biol. Chem. *276*, 44936–44943.

Dervan, P.B. (2001). Molecular recognition of DNA by small molecules. Bioorg. Med. Chem. *9*, 2215–2235.

Dickinson, L.A., Trauger, J.W., Baird, E.E., Dervan, P.B., Graves, B.J., and Gottesfeld, J.M. (1999). Inhibition of Ets-1 DNA binding and ternary complex formation between Ets-1, NF-kappaB, and DNA by a designed DNA-binding ligand. J Biol Chem *274*, 12765-73.

Dutta, P., Bui, T., Bauckman, K.A., Keyomarsi, K., Mills, G.B., and Nanjundan, M. (2013). EVI1 splice variants modulate functional responses in ovarian cancer cells. Mol. Oncol. *7*, 647–668.

Firat, E., Weyerbrock, A., Gaedicke, S., Grosu, A.L., and Niedermann, G. (2012). Chloroquine or chloroquine-PI3K/Akt pathway inhibitor combinations strongly promote γ-irradiation-induced cell death in primary stem-like glioma cells. PLoS ONE *7*, e47357.

Geierstanger, B.H., Mrksich, M., Dervan, P.B., and Wemmer, D.E. (1994). Design of a G.C-specific DNA minor groove-binding peptide. Science *266*, 646–650.

Glass, C., Wuertzer, C., Cui, X., Bi, Y., Davuluri, R., Xiao, Y.Y., Wilson, M., Owens, K., Zhang, Y., and Perkins, A. (2013). Global identification of EVI1 target genes in acute myeloid leukemia. PLoS ONE *8*, e67134.

Gómez-Benito, M., Conchillo, A., García, M.A., Vázquez, I., Maicas, M., Vicente, C., Cristobal, I., Marcotegui, N., García-Ortí, L., Bandrés, E., et al. (2010). EVI1 controls proliferation in acute myeloid leukaemia through modulation of miR-1-2. Br. J. Cancer *103*, 1292–1296.

Goyama, S., Yamamoto, G., Shimabe, M., Sato, T., Ichikawa, M., Ogawa, S., Chiba, S., and Kurokawa, M. (2008). Evi-1 is a critical regulator for hematopoietic stem cells and transformed leukemic cells. Cell Stem Cell *3*, 207–220.

Han, Y.W., Kashiwazaki, G., Morinaga, H., Matsumoto, T., Hashiya, K., Bando, T., Harada, Y., and Sugiyama, H. (2013). Effect of single pyrrole replacement with β-alanine on DNA binding affinity and sequence specificity of hairpin pyrrole/imidazole polyamides targeting 5′-GCGC-3′. Bioorg. Med. Chem. *21*, 5436–5441.

Hargrove, A.E., Raskatov, J.A., Meier, J.L., Montgomery, D.C., and Dervan, P.B. (2012). Characterization and solubilization of pyrrole-imidazole polyamide aggregates. J. Med. Chem. *55*, 5425–5432.

Hoyt, P.R., Bartholomew, C., Davis, A.J., Yutzey, K., Gamer, L.W., Potter, S.S., Ihle, J.N., and Mucenski, M.L. (1997). The Evi1 proto-oncogene is required at midgestation for neural, heart, and paraxial mesenchyme development. Mech. Dev. *65*, 55–70.

Huang, G.-J., Ben-David, E., Tort Piella, A., Edwards, A., Flint, J., and Shifman, S. (2012). Neurogenomic evidence for a shared mechanism of the antidepressant effects of exercise and chronic fluoxetine in mice. PLoS ONE *7*, e35901.

Izutsu, K., Kurokawa, M., Imai, Y., Maki, K., Mitani, K., and Hirai, H. (2001). The corepressor CtBP interacts with Evi-1 to repress transforming growth factor beta signaling. Blood *97*, 2815–2822.

Jazaeri, A.A., Ferriss, J.S., Bryant, J.L., Dalton, M.S., and Dutta, A. (2010). Evaluation of EVI1 and EVI1s (Delta324) as potential therapeutic targets in ovarian cancer. Gynecol. Oncol. *118*, 189–195.

Kang, J.S., Meier, J.L., and Dervan, P.B. (2014). Design of sequence-specific DNA binding molecules for DNA methyltransferase inhibition. J. Am. Chem. Soc. *136*, 3687–3694.

Kilbey, A., Stephens, V., and Bartholomew, C. (1999). Loss of cell cycle control by deregulation of cyclin-dependent kinase 2 kinase activity in Evi-1 transformed fibroblasts. Cell Growth Differ. *10*, 601–610.

Konantz, M., André, M.C., Ebinger, M., Grauer, M., Wang, H., Grzywna, S., Rothfuss, O.C., Lehle, S., Kustikova, O.S., Salih, H.R., et al. (2013). EVI-1 modulates leukemogenic potential and apoptosis sensitivity in human acute lymphoblastic leukemia. Leukemia *27*, 56–65.

Liu, Y., Chen, L., Ko, T.C., Fields, A.P., and Thompson, E.A. (2006). Evi1 is a survival factor which conveys resistance to both TGFbeta- and taxol-mediated cell death via PI3K/AKT. Oncogene *25*, 3565–3575.

Lugthart, S., van Drunen, E., van Norden, Y., van Hoven, A., Erpelinck, C.A.J., Valk, P.J.M., Beverloo, H.B., Löwenberg, B., and Delwel, R. (2008). High EVI1 levels predict adverse outcome in acute myeloid leukemia: prevalence of EVI1 overexpression and chromosome 3q26 abnormalities underestimated. Blood *111*, 4329–4337.

Maicas, M., Vázquez, I., Vicente, C., García-Sánchez, M.A., Marcotegui, N., Urquiza, L., Calasanz, M.J., and Odero, M.D. (2013). Functional characterization of the promoter region of the human EVI1 gene in acute myeloid leukemia: RUNX1 and ELK1 directly regulate its transcription. Oncogene *32*, 2069–2078.

Matsuda, H., Fukuda, N., Ueno, T., Tahira, Y., Ayame, H., Zhang, W., Bando, T., Sugiyama, H., Saito, S., Matsumoto, K., et al. (2006). Development of gene silencing pyrrole-imidazole polyamide targeting the TGF-β1 promoter for treatment of progressive renal diseases. J. Am. Soc. Nephrol. *17*, 422–432.

Meier, J.L., Montgomery, D.C., and Dervan, P.B. (2012a). Enhancing the cellular uptake of Py-Im polyamides through next-generation aryl turns. Nucleic Acids Res. *40*, 2345–2356.

Meier, J.L., Yu, A.S., Korf, I., Segal, D.J., and Dervan, P.B. (2012b). Guiding the design of synthetic DNA-binding molecules with massively parallel sequencing. J. Am. Chem. Soc. *134*, 17814–17822.

Morishita, K., Parganas, E., William, C.L., Whittaker, M.H., Drabkin, H., Oval, J., Taetle, R., Valentine, M.B., and Ihle, J.N. (1992). Activation of EVI1 gene expression in human acute myelogenous leukemias by translocations spanning 300–400 kilobases on chromosome band 3q26. Proc. Natl. Acad. Sci. USA *89*, 3937–3941.

Mucenski, M.L., Taylor, B.A., Ihle, J.N., Hartley, J.W., Morse, H.C., 3rd, Jenkins, N.A., and Copeland, N.G. (1988). Identification of a common ecotropic viral integration site, Evi-1, in the DNA of AKXD murine myeloid tumors. Mol. Cell. Biol. *8*, 301–308.

Murty, M.S., and Sugiyama, H. (2004). Biology of N-methylpyrrole-N-methylimidazole hairpin polyamide. Biol. Pharm. Bull. *27*, 468–474.

Muzikar, K.A., Nickols, N.G., and Dervan, P.B. (2009). Repression of DNA-binding dependent glucocorticoid receptor-mediated gene expression. Proc. Natl. Acad. Sci. USA *106*, 16598–16603.

Nayak, K.B., Kuila, N., Das Mohapatra, A., Panda, A.K., and Chakraborty, S. (2013). EVI1 targets ΔNp63 and upregulates the cyclin dependent kinase inhibitor p21 independent of p53 to delay cell cycle progression and cell proliferation in colon cancer cells. Int. J. Biochem. Cell Biol. *45*, 1568–1576.

Nickols, N.G., and Dervan, P.B. (2007). Suppression of androgen receptor-mediated gene expression by a sequence-specific DNA-binding polyamide. Proc. Natl. Acad. Sci. USA *104*, 10418–10423.

Nickols, N.G., Szablowski, J.O., Hargrove, A.E., Li, B.C., Raskatov, J.A., and Dervan, P.B. (2013). Activity of a Py-Im polyamide targeted to the estrogen response element. Mol. Cancer Ther. *12*, 675–684.

Patel, J.B., Appaiah, H.N., Burnett, R.M., Bhat-Nakshatri, P., Wang, G., Mehta, R., Badve, S., Thomson, M.J., Hammond, S., Steeg, P., et al. (2011). Control of EVI-1 oncogene expression in metastatic breast cancer cells through microRNA miR-22. Oncogene *30*, 1290–1301.

Pradhan, A.K., Mohapatra, A.D., Nayak, K.B., and Chakraborty, S. (2011). Acetylation of the proto-oncogene EVI1 abrogates Bcl-xL promoter binding and induces apoptosis. PLoS ONE *6*, e25370.

Sitailo, S., Sood, R., Barton, K., and Nucifora, G. (1999). Forced expression of the leukemia-associated gene EVI1 in ES cells: a model for myeloid leukemia with 3q26 rearrangements. Leukemia *13*, 1639–1645.

Soderholm, J., Kobayashi, H., Mathieu, C., Rowley, J.D., and Nucifora, G. (1997). The leukemia-associated gene MDS1/EVI1 is a new type of GATA-binding transactivator. Leukemia *11*, 352–358.

Subramanian, A., Tamayo, P., Mootha, V.K., Mukherjee, S., Ebert, B.L., Gillette, M.A., Paulovich, A., Pomeroy, S.L., Golub, T.R., Lander, E.S., and Mesirov, J.P. (2005). Gene set enrichment analysis: a knowledge-based approach for interpreting genome-wide expression profiles. Proc. Natl. Acad. Sci. USA *102*, 15545–15550.

Takahashi, T., Asami, Y., Kitamura, E., Suzuki, T., Wang, X., Igarashi, J., Morohashi, A., Shinojima, Y., Kanou, H., Saito, K., et al. (2008). Development of pyrrole-imidazole polyamide for specific regulation of human aurora kinase-A and -B gene expression. Chem. Biol. *15*, 829–841.

Tanaka, M., Suzuki, H.I., Shibahara, J., Kunita, A., Isagawa, T., Yoshimi, A., Kurokawa, M., Miyazono, K., Aburatani, H., Ishikawa, S., and Fukayama, M. (2014). EVI1 oncogene promotes KRAS pathway through suppression of microRNA-96 in pancreatic carcinogenesis. Oncogene *33*, 2454–2463.

Trauger, J.W., Baird, E.E., and Dervan, P.B. (1996). Recognition of DNA by designed ligands at subnanomolar concentrations. Nature *382*, 559–561.

Ueno, T., Fukuda, N., Tsunemi, A., Yao, E.-H., Matsuda, H., Tahira, K., Matsumoto, T., Matsumoto, K., Matsumoto, Y., Nagase, H., et al. (2009). A novel gene silencer, pyrrole-imidazole polyamide targeting human lectin-like oxidized low-density lipoprotein receptor-1 gene improves endothelial cell function. J. Hypertens. *27*, 508–516.

Wang, X., Nagase, H., Watanabe, T., Nobusue, H., Suzuki, T., Asami, Y., Shinojima, Y., Kawashima, H., Takagi, K., Mishra, R., et al. (2010). Inhibition of MMP-9 transcription and suppression of tumor metastasis by pyrrole-imidazole polyamide. Cancer Sci. *101*, 759–766.

Wang, T.Y., Huang, Y.P., and Ma, P. (2014). Correlations of common polymorphism of EVI-1 gene targeted by miRNA-206/133b with the pathogenesis of breast cancer. Tumour Biol. Published online June 17, 2014. http://dx.doi.org/10.1007/s13277-014-2213-5.

Warren, C.L., Kratochvil, N.C.S., Hauschild, K.E., Foister, S., Brezinski, M.L., Dervan, P.B., Phillips, G.N., Jr., and Ansari, A.Z. (2006). Defining the sequence-recognition profile of DNA-binding molecules. Proc. Natl. Acad. Sci. USA *103*, 867–872.

Weber-Mangal, S., Sinn, H.-P., Popp, S., Klaes, R., Emig, R., Bentz, M., Mansmann, U., Bastert, G., Bartram, C.R., and Jauch, A. (2003). Breast cancer in young women (< or = 35 years): Genomic aberrations detected by comparative genomic hybridization. Int. J. Cancer *107*, 583–592.

Wessels, L.F.A., van Welsem, T., Hart, A.A.M., van't Veer, L.J., Reinders, M.J.T., and Nederlof, P.M. (2002). Molecular classification of breast carcinomas by comparative genomic hybridization: a specific somatic genetic profile for BRCA1 tumors. Cancer Res. *62*, 7110–7117.

White, S., Baird, E.E., and Dervan, P.B. (1996). Effects of the A.T/T.A degeneracy of pyrrole-imidazole polyamide recognition in the minor groove of DNA. Biochemistry *35*, 12532–12537.

White, S., Baird, E.E., and Dervan, P.B. (1997). Orientation preferences of pyrrole-imidazole polyamides in the minor groove of DNA. J. Am. Chem. Soc. *119*, 8756–8765.

White, D.J., Unwin, R.D., Bindels, E., Pierce, A., Teng, H.Y., Muter, J., Greystoke, B., Somerville, T.D., Griffiths, J., Lovell, S., et al. (2013). Phosphorylation of the leukemic oncoprotein EVI1 on serine 196 modulates DNA binding, transcriptional repression and transforming ability. PLoS ONE *8*, e66510.

Wieser, R. (2007). The oncogene and developmental regulator EVI1: expression, biochemical properties, and biological functions. Gene *396*, 346–357.

Willis, B., and Arya, D.P. (2010). Triple recognition of B-DNA by a neomycin-Hoechst 33258-pyrene conjugate. Biochemistry *49*, 452–469.

Yang, F., Nickols, N.G., Li, B.C., Marinov, G.K., Said, J.W., and Dervan, P.B. (2013). Antitumor activity of a pyrrole-imidazole polyamide. Proc. Natl. Acad. Sci. USA *110*, 1863–1868.

Yuasa, H., Oike, Y., Iwama, A., Nishikata, I., Sugiyama, D., Perkins, A., Mucenski, M.L., Suda, T., and Morishita, K. (2005). Oncogenic transcription factor Evi1 regulates hematopoietic stem cell proliferation through GATA-2 expression. EMBO J. *24*, 1976–1987.

Zhang, Y., Sicot, G., Cui, X., Vogel, M., Wuertzer, C.A., Lezon-Geyda, K., Wheeler, J., Harki, D.A., Muzikar, K.A., Stolper, D.A., et al. (2011). Targeting a DNA binding motif of the EVI1 protein by a pyrrole-imidazole polyamide. Biochemistry *50*, 10431–10441.

